Title: Experimental and Numerical Study of Furniture Fires in an ISO-Room for Use in a Fire Forecasting Framework

Author names and affiliations: Tarek Beji[a], Steven Verstockt[b], Rik Van de Walle[b], Bart Merci[a]

[a] Ghent University – UGent, Dept. Flow, Heat and Combustion Mechanics, Sint-Pietersnieuwstraat 41, B-9000 Ghent, Belgium

[b] Dept. Electronics and Information Systems, Multimedia Lab, Ghent University – IBBT, Gaston Crommenlaan 8, Bus 201, B-9050 Ledeberg-Ghent, Belgium

E-mail addresses of the authors:

1. Tarek Beji: Tarek.Beji@UGent.be

2. Steven Verstockt: Steven.Verstockt@howest.be

3. Rik Van de Walle: rik.vandewalle@UGent.be

4. Bart Merci: Bart.Merci@UGent.be

Corresponding author:

Dr. Tarek Beji

Ghent University – UGent, Department of Flow, Heat and Combustion Mechanics, St. Pietersnieuwstraat 41

Tel : ++32 9 264 98 46; Fax : ++32 9 264 35 75

E-mail: Tarek.Beji@UGent.be

Biography of authors

Tarek Beji is a postdoctoral researcher at the University of Ghent (Belgium) in the group of Prof. Bart Merci. He received his PhD from the University of Ulster (United Kingdom) in Fire Engineering in 2009. Since 2006 he has been working in the areas of enclosure fires and soot modelling.

Steven Verstockt received his Master degree in Informatics from Ghent University in 2003. At the end of 2007 he joined the ELIT Lab of the University College West-Flanders as a researcher. In 2008, he started a PhD on video fire analysis at the Multimedia Lab of the Department of Electronics and Information Systems of Ghent University - IBBT (Belgium). Since 2012 he works as a post-doctoral researcher in this lab. His research interests include video surveillance, computer vision and multi-sensor data fusion.

Rik Van de Walle received his M.Sc. and PhD degrees in Engineering from Ghent University, Belgium in 1994 and 1998 respectively. After a visiting scholarship at the University of Arizona (Tucson, USA), he returned to Ghent University, where he became professor of multimedia systems and applications, and head of the Multimedia Lab. His current research interests include multimedia content delivery, presentation and archiving, coding and description of multimedia data, content adaptation, and interactive (mobile) multimedia applications.

Bart Merci received his Master degree in Electro-Mechanical Engineering at Ghent University, Belgium, in 1997. He obtained his Ph.D. degree (topic: numerical simulations of turbulent combustion) at the Faculty of Engineering and Architecture at Ghent University in 2000. He became Professor in 2004 and is now the Head of the research unit 'Combustion, Fire and Fire Safety' at this Faculty. His research interests include fire safety engineering, as well as turbulence-chemistry interaction in turbulent flames.

Experimental and Numerical Study of Furniture Fires in an ISO-Room for Use in a Fire Forecasting Framework

ABSTRACT

The proposed method of forecasting a single-room fire growth based on inverse modelling relies upon the assimilation of temperature measurements at the doorway level, from floor to soffit height. These measurements are processed in the context of a two-zone model to obtain transient profiles of neutral plane height, X_N, and upper layer temperature, T_u. An additional correlation is used to deduce the smoke layer height, h, within the fire room. The obtained profiles of T_u, X_N and h over a given period of time (the 'assimilation window') are used to estimate the fire growth factor, α, the time delay, t_0, and the heat loss factor, λ_c, with a two-zone inverse modelling procedure. Instantaneous displays of the future fire development are then delivered. Experimental data of four furniture fires in an ISO room are analyzed to illustrate the proposed forecasting methodology, which provides positive lead times between 20 and 235 s, depending on the fire growth rate.

KEYWORDS

Single-room fire experiments, fire forecasting, inverse modelling, two-zone model

INTRODUCTION

In order to assist a decision support system and fire service intervention when a fire takes place in a building, the concept of fire forecasting has been introduced and described in [1-3]. It consists of displaying future hazards (*e.g.* smoke levels, flashover occurrence or structural collapse) using assimilation of live data into a fire model. The available computational resources

and the required computational times render the use of CFD fire models for forecasting purposes (*i.e.* real-time predictions) practically impossible for the time being. A two-zone modelling approach remains the most efficient solution because it is substantially faster [4]. In complex geometries, it may be necessary to apply CFD, but in the simple geometry addressed in the present paper (ISO room [5]), two-zone models are applicable.

The fire forecasting concept includes an optimization part to find the fire parameters (*e.g.* size and location) which give the best match with the observed data provided by the sensing system. The solution to this inverse problem is obtained by developing an Inverse Fire Modelling (IFM) framework. Table 1 provides several IFM frameworks that have been developed for a number of fire scenarios, using different optimization techniques. Table 1 shows that the first and most important parameter to be estimated is the HRR (steady or transient). In most frameworks [2-3, 6, 8, 13], this is performed by analyzing temperature and/or smoke measurements. This is also the case for the work presented in this paper. An alternate approach has been developed in [14]. It consists of reconstructing the HRR profile from video recordings of flame dimensions obtained with the means of a flame detection algorithm. A projection of the HRR is then fed into a two-zone model to produce forecasts of upper layer temperature and smoke layer height. This video-based approach is not used in this paper. However, video measurements of smoke interface height are provided here and compared to measurements of h obtained from temperature recordings in order to evaluate and validate the smoke detection algorithm [14-15] for future applications.

As stated earlier, obtaining reliable real-time predictions (*i.e.* predictions with positive lead times) is a *sine qua non* condition in a fire forecasting context. The efficiency of an IFM framework in this regard is strongly dependent on the optimization (*i.e.* inverse modelling) procedure. For example, Neviackas and Trouvé [8] used a Genetic Algorithm (GA) to find the

HRR (and other parameters related to the geometry of the vents) from upper layer temperature measurements. They stated that "GAs provide an excellent numerical performance in high dimensional problems. However, simulation times (1-1.5 hours for a single compartment and 6-7 hours for multi-compartments) must be drastically reduced". Koo et al. [11] used large-scale fire measurements and a Monte-Carlo approach to predict fire development using zone model simulations. However, they did not report positive lead times. In [2-3] positive lead times were reported. A gradient-based technique, namely the tangent linear technique, was applied to the case of a radially growing (alpha-t^2 fire) in an adiabatic closed compartment with leaks. Despite the encouraging results, the scenario considered in [2-3] remains an idealized fire scenario. The authors underlined the necessity of adding further realism in future studies. Furthermore, it has been pointed out that the gradient-based method might lead to convergence problems. The method proposed in [13] relies upon an iterative procedure (without convergence problems) that allows reconstructing transient HRR profiles from temperature measurements (obtained during actual fire experiments) using CFAST [7] simulations. The method has been proven to provide reliable inverse HRR solutions. However, it has not been applied for forecasting purposes, which implies (1) running the inverse modelling method over a limited period of time, (2) estimating the HRR (and possibly other unknowns) evolution with time, and then (3) producing a forecast. Furthermore, only temperature measurements are taken into account, the smoke interface height is not accounted for. The intent of the present paper is to cope with these issues by proposing a method, which provides positive lead times, based solely on temperature measurements at the doorway (processed to obtain smoke interface and average layer temperature). Multiple measurements within the fire room are thus not required. The data of four furniture fire experiments, carried out in an ISO-room [5] with an open doorway, are analyzed to illustrate the method.

Table 1. Previous studies on Inverse Modelling and Fire Forecasting.

Reference	**Fire Scenario**			**IFM**				
	Geometry	*CFD Zone model Actual Exp.*	*HRR*	*Fire Model*	*Optimization Method*	*Assimilated data*	*MI(s)*	*Simulation time*
Davis et al. (2001) [6]	Multiple compartments	Actual Exp.	Methane burner / wood pallets	Zone Model: CFAST [7]	Algebraic equation + estimates	Ceiling temperature	HRR	Instantaneous
Neviackas et al. (2007) [8]	Single compartment + door and/or window	FDS [9] or BRI2002[10]	Constant	Zone Model: BRI2002 [10]	Genetic Algorithm	Upper layer temperature	HRR, vent configuration	1-1.5 hours on a single 2.0 GHz processor
Neviaskas et al. (2007) [8]	Multiple compartments (18)	FDS [9]	Constant	Zone Model: BRI2002 [10]	Genetic Algorithm	Upper layer temperature	HRR, door widths	6-7 hours on a single 2.0 GHz processor
Koo et al. (2010) [11]	Multiple compartments	Actual Exp.	Furniture fire	Zone Model: CRISP	Selection from several scenarios using the Monte Carlo method	temperature	Not specified	Negative lead times
Jahn et al. (2010) [2-3]	Single closed compartment with floor leakage	FDS [9]	α-t^2 fire	Zone Model [12]	Tangent Linear Model (TLM)	Upper layer temperature + smoke layer height (inside the enclosure)	Fire growth factor: α Entrainment coeff.: C	Faster than real-time
Overholt et al. (2012) [13]	Single compartments + door	CFAST data + Actual Exp.	Steady and transient	CFAST [7]	Iterative gradient-free method	T_u (inside the enclosure)	HRR	5 to 10 s
Beji et al. (2012) [14]	ISO-room with open doorway	Actual Exp.	Sofa fire	Simplified zone model [14]	-	Flame dimensions	-	Instantaneous

The experimental design is described in the following section. Then, the two-zone model is presented. The obtained experimental data are processed and analyzed accordingly. After validation of the forward model (*i.e.* two-zone model), a description of the inverse modelling framework and an application of the methodology are provided and discussed before drawing the main conclusions.

EXPERIMENTAL DESIGN

Four experiments have been conducted in an ISO-room [5] (dimensions: 3.6 m × 2.4 m × 2.4 m high) with walls and ceiling made of lightweight concrete. Figures 1 and 2 show a display of the overall arrangement, including the positioning of thermocouples and a video camera. Natural ventilation induced flows occur through a single open doorway (0.8 m by 2.0 m high). Wooden chairs and sofas have been placed in several positions. More details are provided in Table 2.

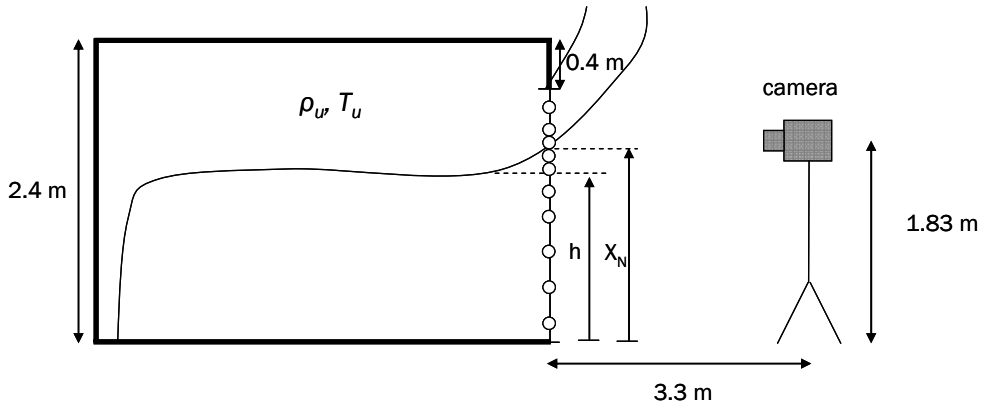

Figure 1. Experimental set-up: geometry and positioning of the thermocouples and the camera. The solid points in the middle of the doorway are thermocouples placed at respectively, 0.02m, 0.32m, 0.62m, 0.92m, 1.12m, 1.32m, 1.42m, 1.52m, 1.62m, and 1.82m above floor level.

Table 2. Description of tests.

Test N°	Burning items	Position	Ignition
1	4 wooden chairs + small cushion	centre	2 ignited baskets of wood saw dusts
2	4 wooden chairs + small cushion	corner	2 ignited baskets of wood saw dusts
3	2-seat sofa + cushions	against back wall	Small wood cribs [a]
4	3-seat sofa + cushions	against back wall	Small wood cribs [a]

[a] *soaked in liquid fuel*

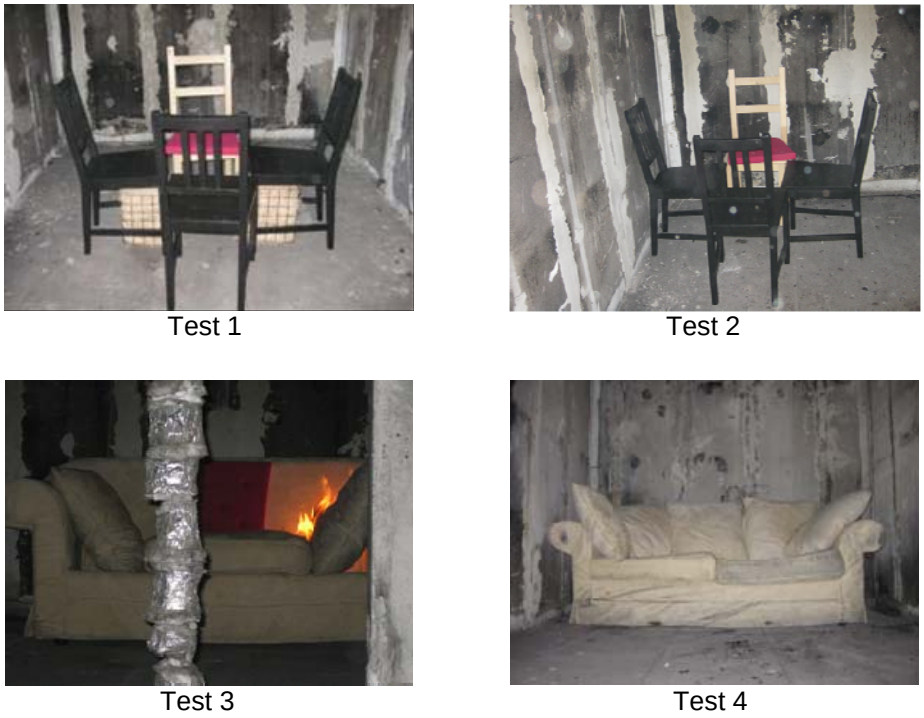

Figure 2. Picture of the fuel packages used for each test.

The heat release rate (HRR), calculated using oxygen depletion calorimetry, has been recorded every 5 s. A smoke detection algorithm [14-15] (using video data) provides measurements of the smoke layer height every 5 s. Temperatures at the doorway have been recorded every 5 s. The experimental results are presented and analyzed hereafter in the context of two-zone modelling. Therefore, a brief description of the two-zone fire model is provided first.

TWO-ZONE FIRE MODELLING

As described in [14, 17], only the basic equations of mass and energy conservation for the hot upper layer are solved in conjunction with sub-models for plume entrainment and mass flow rate of hot gas out of the doorway.

Conservation equations

The energy conservation equation reads:

$$\frac{d}{dt}\left[\rho_u c_p \left(T_u - T_a\right) A\left(H - h\right)\right] = \dot{Q}_{net} - \dot{m}_{out,u}\, c_p \left(T_u - T_a\right) \tag{1}$$

where t is the time, ρ_u the upper layer density, c_p the specific heat of air, T_u the upper layer temperature, T_a the ambient temperature, A the surface area of the room and H its height. The variables $\dot{Q}_{net}$ and $\dot{m}_{out,u}$ denote respectively the net HRR and the mass flow rate of hot gases through the door opening.

The density is calculated from temperature, through the ideal law:

$$\rho = \frac{353}{T} \tag{2}$$

The net HRR is expressed as a function of the total HRR, $\dot{Q}_f$ according to:

$$\dot{Q}_{net} = (1 - \lambda_c)\dot{Q}_f \tag{3}$$

where λ_c is the fraction of energy released by the fire that is not absorbed by the upper layer. In other words it represents the boundary heat losses. This fraction is assumed to be constant as in other fire models [16-17]. Cooper [18] suggests values for λ_c in the range of 0.6 to 0.9 for most situations [19]. Mowrer [20] reported a value of 0.7 for a series of fire tests in a relatively large room. Hammins et al [21] found that nearly 74% of the fire energy went to compartment surfaces

for the case of an enclosure designed to represent a realistic-scale cable room in a nuclear power plant. As pointed out by Mowrer [20], temperature predictions are sensitive to the selection of λ_c and further work is needed to characterize appropriate heat loss factors for a range of enclosure geometries, boundary materials, surface conditions and fire sizes and durations.

The mass conservation equation for the upper layer reads:

$$\frac{d}{dt}\left(\rho_u A\left(H-h\right)\right) = \dot{m}_p + \dot{m}_{in,u} - \dot{m}_{out,u} \tag{4}$$

where $\dot{m}_p$ is the plume mass flow rate at the bottom side of the upper layer and $\dot{m}_{in,u}$ the mass flow rate of fresh air into the upper layer.

Plume entrainment

Several plume entrainment models have been developed in the past (*e.g.* [22-25]). For the case of room fires, McCaffrey's model [22] was implemented in CFAST and validated for a series of experiments [7]. Furthermore, a comparative study on entrainment models [26] showed that McCaffrey's model gives the best agreement for full-scale compartment fires with rates between 330 kW and 980 kW. An additional advantage of this model is that it does not rely upon parameters such as the fire diameter or the flame height. This is an interesting feature for the sake of a simple, yet efficient, formulation of the fire dynamics in an inverse modelling framework. Numerically speaking, it is also easier to estimate 2 parameters than 3 or more.

The model reads:

$$\dot{m}_p = 0.011\,\dot{Q}_f \left(\frac{h-z_f}{\dot{Q}_f^{\,2/5}}\right)^{0.566}, \quad 0 < \frac{h-z_f}{\dot{Q}_f^{\,2/5}} < 0.08 \tag{5a}$$

$$\dot{m}_p = 0.026\ \dot{Q}_f \left(\frac{h - z_f}{\dot{Q}_f^{\,2/5}} \right)^{0.909}, \quad 0.08 < \frac{h - z_f}{\dot{Q}_f^{\,2/5}} < 0.20 \tag{5b}$$

$$\dot{m}_p = 0.124\ \dot{Q}_f \left(\frac{h - z_f}{\dot{Q}_f^{\,2/5}} \right)^{1.895}, \quad 0.20 < \frac{h - z_f}{\dot{Q}_f^{\,2/5}} \tag{5c}$$

where z_f is the elevation of the fire source above floor level.

Vent flow

After a relatively short period (in the order of a few seconds and referred to in [27] as stages A and B), the flow through the doorway becomes bidirectional: hot gases flow out through the top part of the door opening and fresh air enters through the lower part. The flow is stratified. Application of Bernoulli's equation and hydrostatic principles leads to the following equations [27]:

$$\dot{m}_{out,u} = (2/3)\, C_d\, W_D \sqrt{2\, g\, \rho_u (\rho_a - \rho_u)}\, (H_D - X_N)^{3/2} \tag{6a}$$

$$\dot{m}_{in,u} = (2/3)\, C_d\, W_D \sqrt{2\, g\, \rho_a (\rho_a - \rho_u)}\, (X_N - h)^{3/2} \tag{6b}$$

$$\dot{m}_{in,l} = C_d\, W_D\, h \sqrt{2\, g\, \rho_a (\rho_a - \rho_u)(X_N - h)} \tag{6c}$$

where $\dot{m}_{in,l}$ is the mass flow rate of fresh air flowing into the lower layer, C_d is the discharge coefficient, W_D and H_D are respectively, the doorway width and height, g is the gravitational acceleration, and ρ_a and ρ_u are the ambient and the upper layer densities.

Equating the mass flow rates into and out of the room gives [27]:

$$\sqrt{\rho_a (X_N - h)}(X_N + h/2) = \sqrt{\rho_u}(H_D - X_N)^{3/2} \quad (7)$$

In the following section, a validation of the two-zone is provided after presentation of the experimental results.

EXPERIMENTAL RESULTS AND VALIDATION OF THE FIRE MODEL

Experimental results

Temperatures at the doorway, recorded every 5 s, have been processed according to the least-square method described in [28] in order to estimate the neutral plane height, X_N, and the upper layer temperature, T_u, as suggested in [29]. In the least-squares method [28], the lower layer and upper layer temperatures (T_ℓ and T_u) are defined at the doorway as:

$$T_\ell = \frac{1}{X_N} \int_0^{X_N} T\, dz \quad (8a)$$

$$T_u = \frac{1}{H_D - X_N} \int_{X_N}^{H_D} T\, dz \quad (8b)$$

where z is the height and H_D the height of the door.

The idea consists of finding, using an iterative procedure, the value of X_N that minimizes the following function:

$$\sigma^2 = \frac{1}{X_N} \int_0^{X_N} (T - T_\ell)^2\, dz + \frac{1}{H_D - X_N} \int_{X_N}^{H_D} (T - T_u)^2\, dz \quad (9)$$

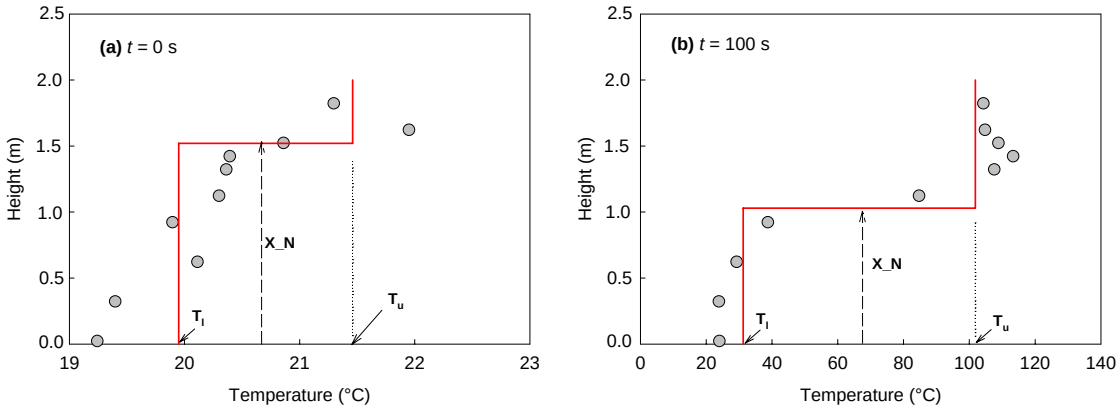

Figure 3. Two-zone post-processing of the temperature data at the doorway for Test 1 at (a) $t = 0$ s (*i.e.* ignition time) and (b) $t = 100$ s.

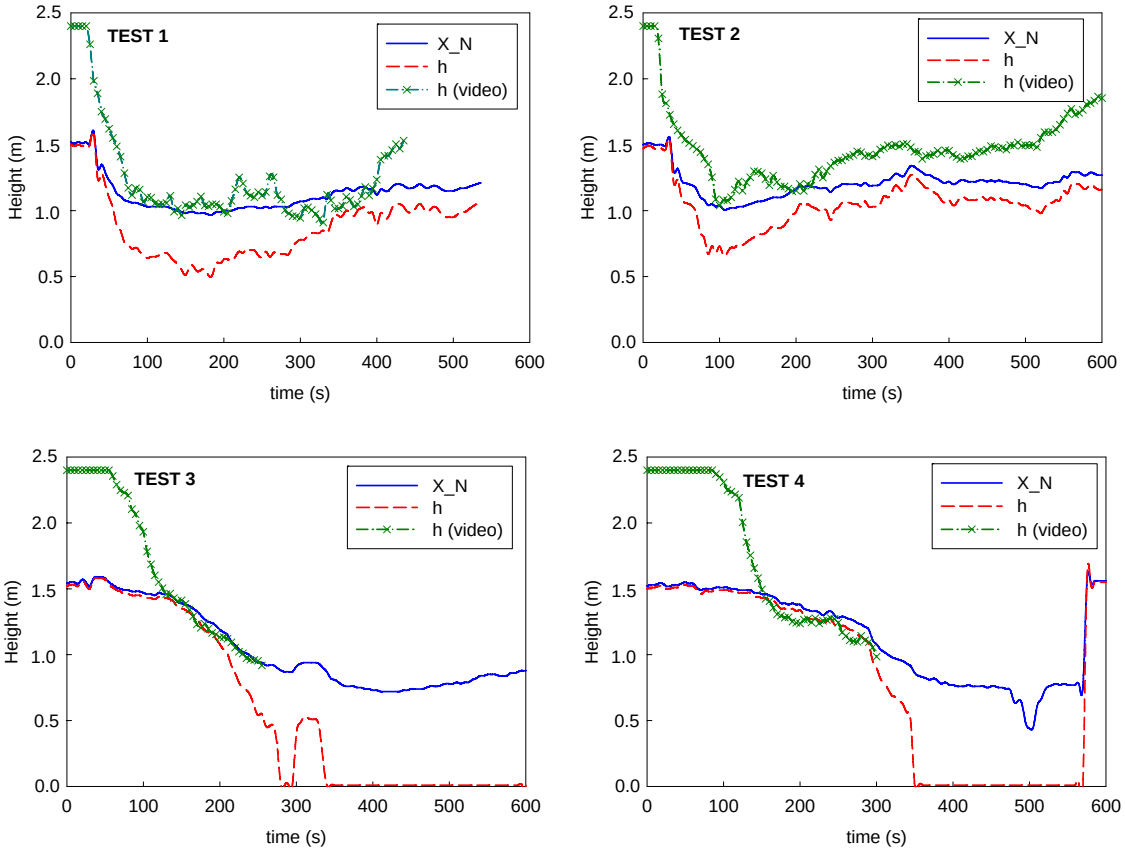

Figure 4. Evolution of the neutral plane height, X_N, and smoke layer height, h, estimated from temperature measurements and the interface height measured by the video camera.

Figure 3 shows the results of the least-square method applied to two instants in time for Test 1. Figure 3a shows that because of the slight variation (between 19 and 22°C) in the vertical profile of temperature at ignition time, the neutral plane height is initially estimated at $X_N = 1.5$ m.

The values of T_u (and thus ρ_u) and X_N are used to determine the smoke layer height, h, by solving Eq. (7) using an iterative procedure. Figure 4 shows the temporal profiles of X_N and h for each test.

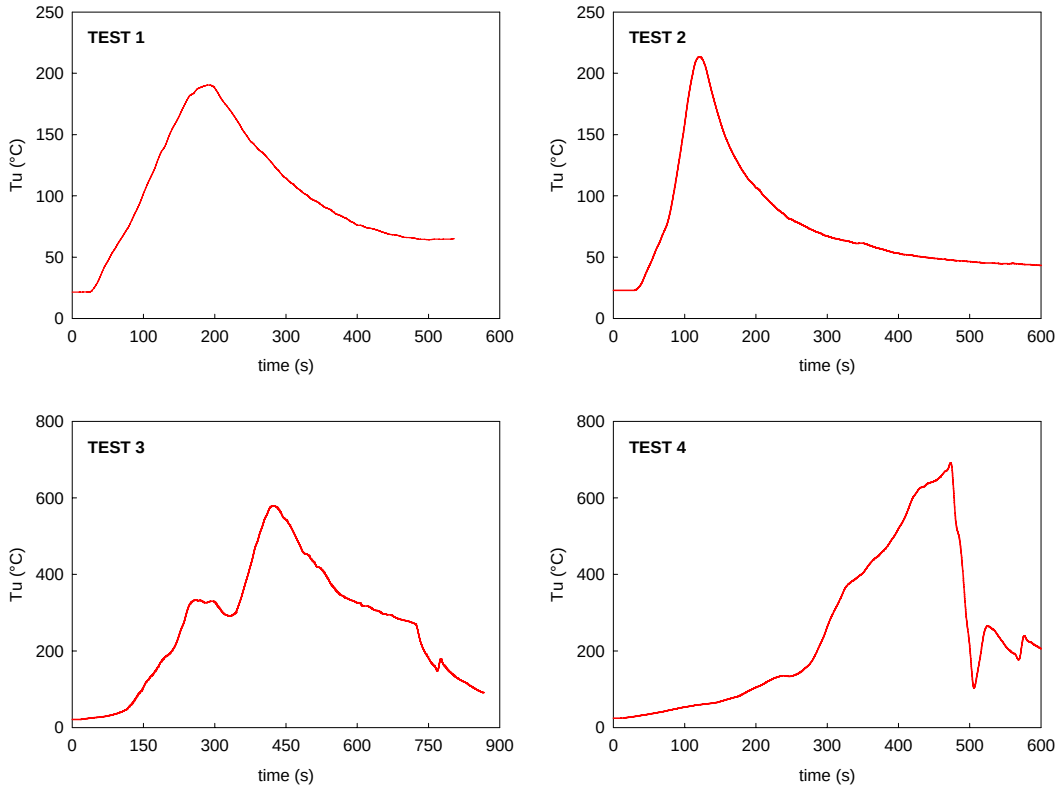

Figure 5. Evolution of the upper layer temperature, T_u, for each test.

Results from the smoke detection algorithm (camera measurements) show that after an initial stage with substantial discrepancies, a good agreement with the thermocouple measurements is obtained, especially for tests 3 and 4 (see Fig. 3). This could be attributed to the higher HRRs (see Fig. 6), which produce hotter and thicker smoke, easier to detect.

In tests 3 and 4 a transition from the stratified stage to the well-mixed stage (*i.e.* h = 0 m) has been observed visually and confirmed by thermocouple measurements (at 300 s for Test 3 and 350 s for Test 4, see Fig. 4). In order to avoid damage to the camera, it was removed just before this stage. Consequently, there are no video measurements of the smoke layer height during and after this transition period.

Figure 5 shows the upper layer temperature profiles for each test.

From the results presented in Figs. 4 and 5, the net HRR, $\dot{Q}_{net}$, has been calculated by discretizing Eq. (1) as follows:

$$\dot{Q}^i_{net} = \dot{m}^i_{out,u}\, c_p (T^i_u - T_a) + \frac{c_p A}{\Delta t}\left[\rho^i_u (T^i_u - T_a)(H - h^i) - \rho^{i-1}_u (T^{i-1}_u - T_a)(H - h^{i-1})\right], \quad i = 2, N_{data} \quad \text{(10a)}$$

where N_{data} is the number of available experimental measurements and $\Delta t = 5\,s$ the recording time.

The mass flow rate of hot gases through the door opening is calculated as:

$$\dot{m}^i_{out,u} = (2/3)\, C_d\, W_D \sqrt{2\, g\, \rho^i_u \left(\rho_a - \rho^i_u\right)} \left(H_D - X^i_N\right)^{3/2} \quad \text{(10b)}$$

Applying Eqs. (10a) and (10b) to the complete set of data provides estimates of the net HRR profile for each test, which are shown in Fig. 6. The comparison between the profiles of the total HRR (measured by oxygen calorimetry) and the net HRR confirm that the heat loss factor can reach values between 50 and 70%.

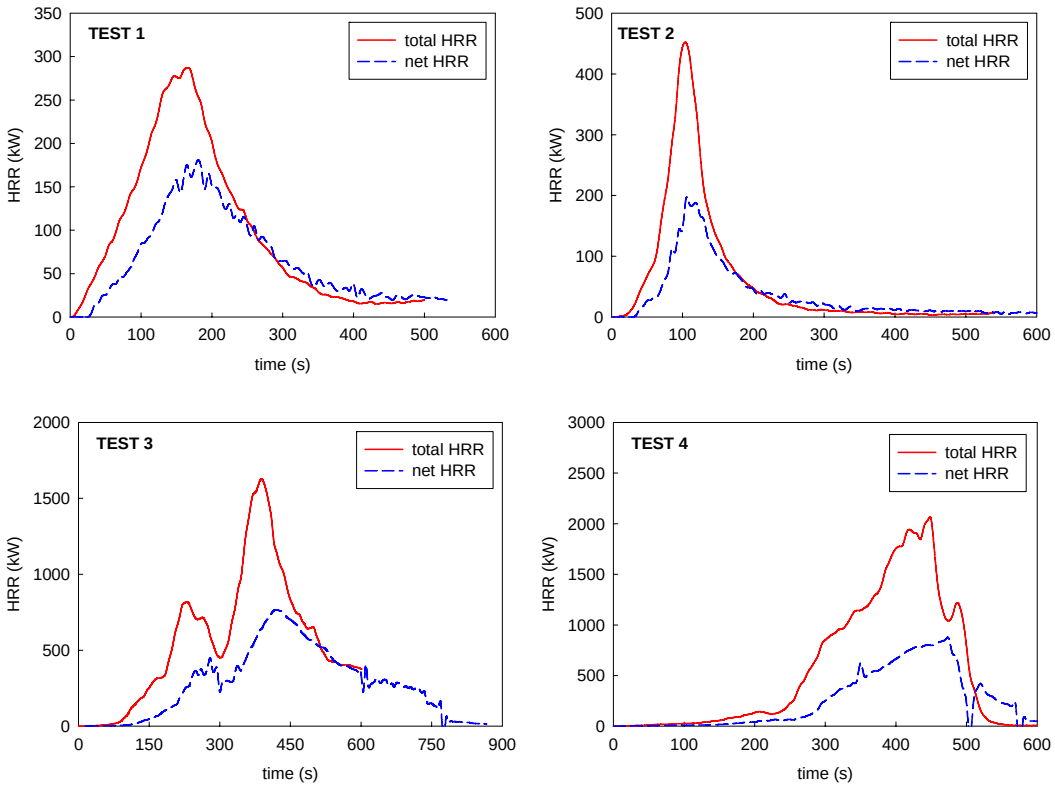

Figure 6. Evolution of the net and total HRR for each test.

Validation of the two-zone model

Before performing any inverse modelling calculations, it must be ensured that the forward model is reliable. This is performed here by providing the HRR measured by oxygen calorimetry as an input. For the remaining unknown, namely the heat loss factor, two values are used: $\lambda_c = 0.5$ and $\lambda_c = 0.7$. These two values were chosen on the basis of the analysis of Fig. 6. Figure 7 shows that the prediction of X_N is not sensitive to the value of λ_c. Obviously, the temperature predictions are sensitive to the value of λ_c. Figure 8 shows that for tests 1 and 2, the heat loss factor is clearly bounded between 0.5 and 0.7 in the fire growth period (and closer to 0.5). For tests 3 and 4, the value of 0.7 seems the most appropriate. Clearly it is relevant to perform further research on the determination of λ_c, depending on the configuration, but for the present study it is sufficient to observe that if the appropriate value of the heat loss factor is chosen, the simple two-zone model

described above provides good predictions of both the neutral plane height and the smoke layer temperature.

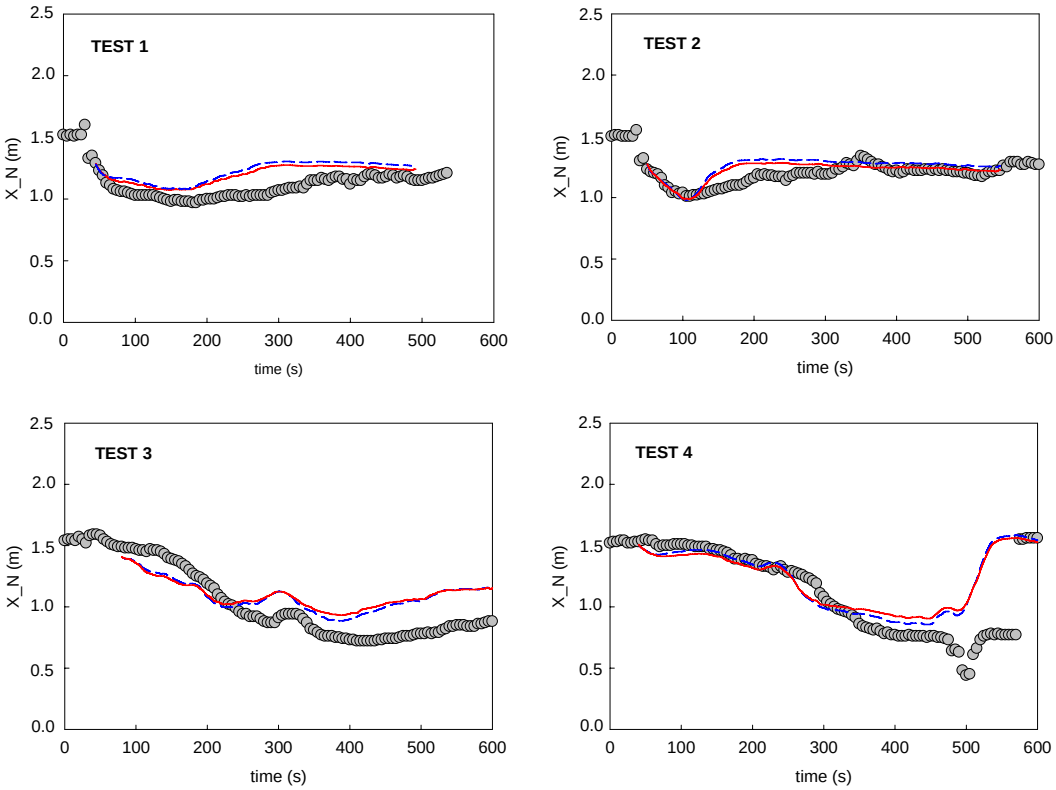

Figure 7. Comparison of the measured profiles (solid points) of the neutral plane height with the predicted profiles using two values for the heat loss factor: $\lambda_c = 0.5$ (solid line) and $\lambda_c = 0.7$ (dashed line).

In the inverse modelling procedure proposed in the following section, the HRR profile and the heat loss factor are not known. Instead they are deduced from the experimental measurements of T_u, X_N and h.

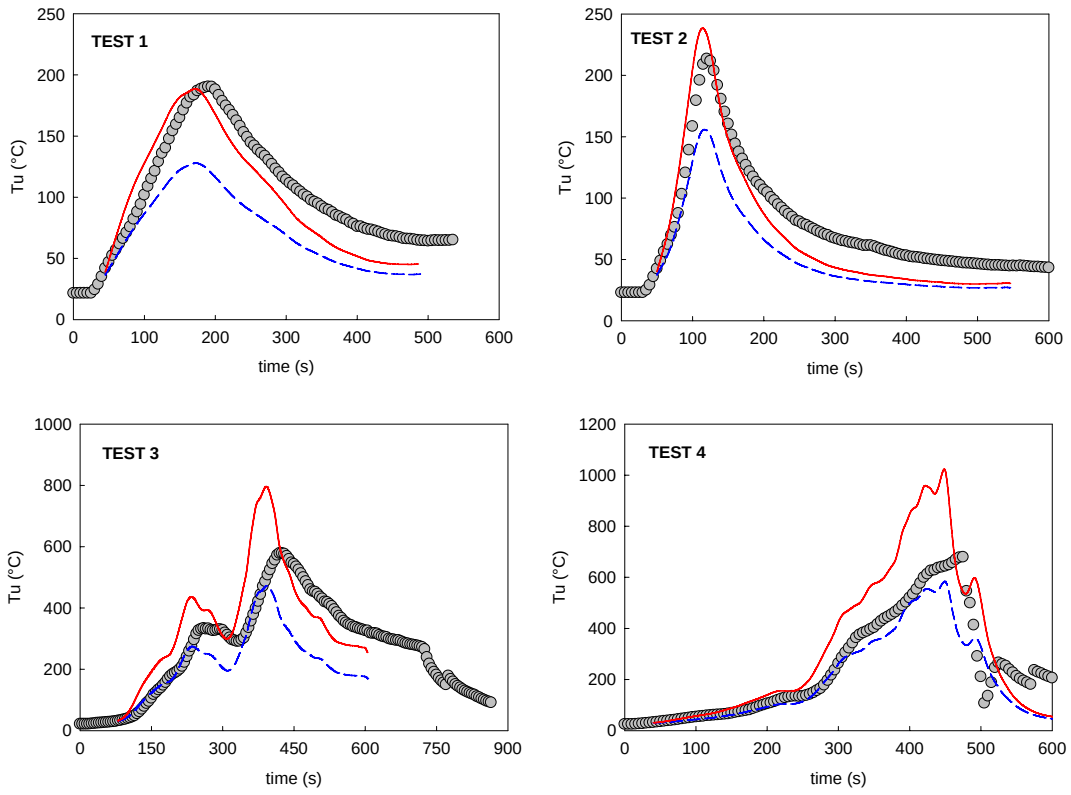

Figure 8. Comparison of the measured profiles (solid points) of the upper layer temperature with the predicted profiles using two values for the heat loss factor $\lambda_c = 0.5$ (solid line) and $\lambda_c = 0.7$ (dashed line).

INVERSE MODELLING

Total and net heat release rate profiles

Several models have been developed and described in the literature in order to characterize heat release rates in fires. If the fire is described as a process of flame spread, where the rate of spread is proportional to the amount of fuel already burning, an "exponential growth" expression is found [30-31]. In the model developed in [32-33], where the burning rate is proportional to the surface of a round flame front with radius proportional to the progress in time, the heat release rate becomes a quadratic function of time. Babrauskas and Walton [34] proposed a triangular

representation of the heat release rate curve for a series of upholstered furniture fires. Such a representation implies a linear fire growth.

In this paper the widely accepted quadratic growth is assumed for all tests. However, an additional inverse modelling procedure using a linear growth is applied for Test 4 in order to investigate the sensitivity of the methodology to the growth model.

The total heat release rate is then expressed as:

$$\dot{Q}_f = \alpha \left(t - t_0 \right)^2 \tag{11}$$

where α is the fire growth factor (in kW/s^2) and t_0 the delay time (in s).

By considering Eq. (3), it is possible to express the net HRR as:

$$\dot{Q}_{net} = \alpha_{net} \left(t - t_0 \right)^2 \tag{12}$$

where the relation between the net and total fire growth factors is:

$$\alpha = \frac{\alpha_{net}}{1 - \lambda_c} \tag{13}$$

As explained earlier, it is possible to estimate the net HRR profile from the measurements of T_u, X_N and h, using Eqs. (10a) and (10b). In the forecasting procedure, this is performed over a limited period of time, namely the 'assimilation window', where the number of data points is between 1 and N. For example, Fig. 9 shows a DA (data assimilation) window of 30 s (between

45 and 75 s after ignition) where the number of data points is $N = 7$. The first data point is not shown because the measurements at 45 s serve as an initial condition to Eqs. (10a) and (10b). Therefore, it is important to mention at this stage that the methodology presented does not require the knowledge of the ignition time. The assimilation procedure could be triggered as soon as a significant change in temperature starts to be recorded at the doorway. In the calculations shown in this work, a threshold of 10°C above ambient was adopted.

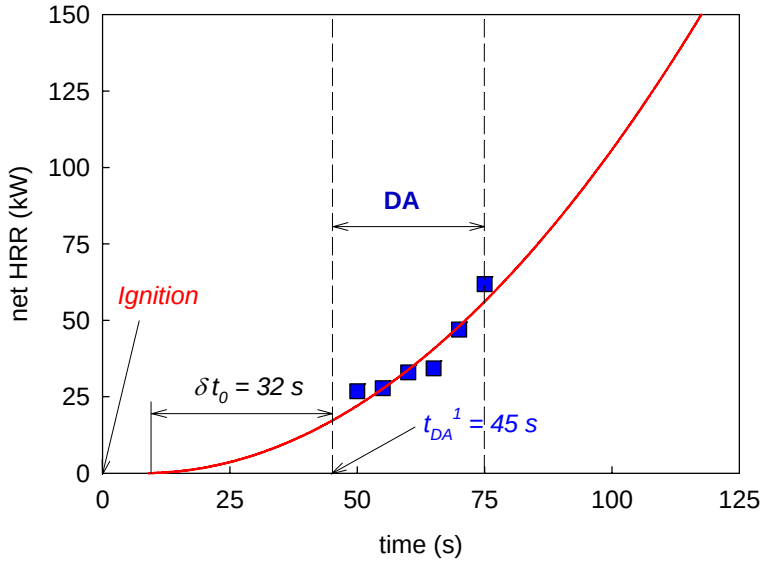

Figure 9. Illustration of the quadratic fire growth fit for Test 2 in order to find α_{net} and t_0.

A fit of the obtained estimations of the net HRR over the assimilation window is performed according to Eq. (12) in order to find α_{net} and t_0 as shown in the example in Fig. 9.

Estimation of the heat loss factor

Previous studies (mentioned above) suggest that λ_c varies in the range of 0.6 to 0.9. However, we consider in this study the wider range [0.00, 0.99]. The two-zone model is run for each possible value of λ_c using a step of 0.01 and the already calculated values of α_{net} and t_0. Such an approach

is possible because the two-zone model calculations are very fast. The deviation between the 'forward model' (*i.e.* the two-zone model) and the 'observed' data is evaluated according to the following cost function (CF):

$$CF = \frac{1}{N}\sum_{i=1}^{N} w\frac{T_{u,i} - \hat{T}_{u,i}}{\hat{T}_{u,i}} + (1-w)\frac{X_{N,i} - \hat{X}_{N,i}}{\hat{X}_{N,i}} \quad (14)$$

where w is a weighting factor taken as 0.5. The superscript ^ denotes the measured value.

The selected value for λ_c is the value that minimizes the cost function and the fire growth factor, α, is deduced from Eq. (13).

Forecast

In order to produce a forecast, no additional run of the forward model is needed. The forecast corresponds to the output of the two-zone model for which the value of the cost function (Eq. (14)) is minimized. As explained earlier, the data assimilation process is triggered when the estimated upper layer temperature is 10°C above ambient. This instant in time is the reference point for all the calculations. However, for the sake of clarity all the results presented in the next section are plotted with the ignition time as reference. Assimilation windows of 30s have been considered. In practice, the window length can be adjusted dynamically, but this is not relevant for the present paper. The calculations of α , t_0 and λ_c are practically instantaneous and thus so is the forecast. The 'quality' of the forecast is constantly evaluated by calculating the deviation between the prediction and the 'newly' collected data. If a systematic underestimation or overestimation by more than 50°C in temperature is observed over a 30 s period of time, the forecast is updated using a new DA window. The lead time (*i.e.* period of time with a good

agreement between the forecast and the observed data) is defined here as the difference between the time of systematic deviation and the time of the display of the forecast (*i.e.* end time of the assimilation window). A similar dynamic procedure has been used in [14] to forecast fire growth in enclosures using real-time video data.

Results

The procedure described above has been applied to the 4 tests. Table 3 provides the list of the DAs performed, and the obtained results in terms of estimated model invariants and lead times.

Table 3. Inverse modelling and forecasting results.

Test	Assimilation window	α_{net} (kW/s^2)	t_0 (s)	λ_c	α (kW/s^2)	t_{lead} (s)
1	[40s; 70s]	0.0069	-47	0.73	0.0257	120
2	[45s; 75s]	0.0125	-32	0.64	0.0347	30
3	[75s; 105s]	0.0108	-52	0.00	0.0108	65
	[155s; 185s]	0.0103	-66	0.53	0.0219	95
4	[35s; 65s]	0.0007	-65	0.00	0.0007	235
	[285s; 315s]	0.0340	-70	0.58	0.0586	20

Results of the forecast for Tests 1 to 4 are shown respectively in Figs. 10 to 13. In these figures, only the fire growth stage (for which the forecast is intended) is shown.

It can be seen in Fig. 10 (test 1) that despite an overestimation of the HRR, the optimized value of the heat loss factor leads to a net HRR that gives a good agreement in the profile of the upper layer temperature with a lead time of 120 s. In a similar way, despite the underestimation of the HRR in Test 2, the optimized value of λ_c results in predictions of T_u with a lead time of 30 s (see Fig. 11). This illustrates that it is not necessary to predict the HRR very accurately to have good

forecasting for temperatures and neutral plane height evolution. Rather, the combination of HRR and heat losses is essential.

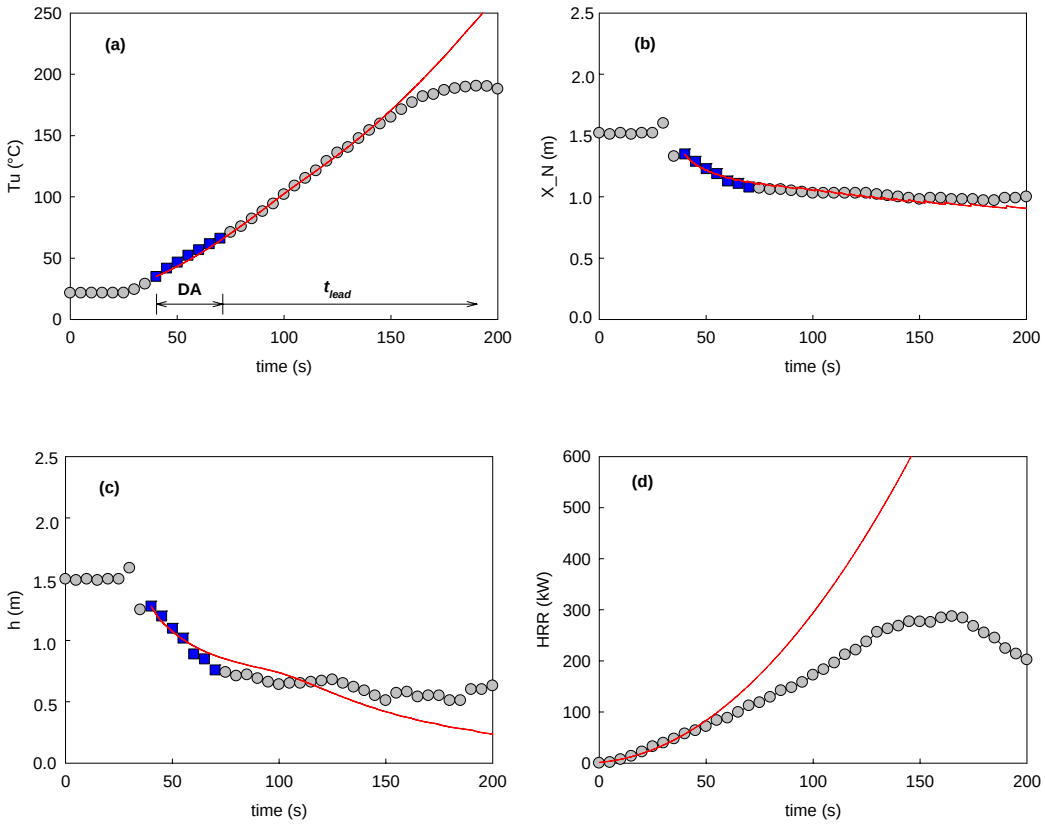

Figure 10. Test 1 fire forecast (solid line). The solid squares are the assimilated data points. The solid points are the remaining experimental data points. (a) Upper layer temperature. (b) Neutral Plane height. (c) Smoke layer height. (d) HRR.

Contrary to Tests 1 and 2, which did not require an update of the forecast during the fire growth stage, two DAs are performed for Tests 3 and 4 in order to capture the change in the trend of the HRR and the subsequent smoke height and temperature profiles.

In Test 3, the first assimilation window considered is [75s; 105s]. The optimized values are: α = 0.0108 kW/s^2, t_0 = -52 s and λ_c = 0.00. From t = 170 s onward the neutral plane height is systematically overestimated and the temperature underestimated by more than 50°C. Therefore, the lead time obtained after the first assimilation is t_{lead} = 170 – 105 s = 65 s. A new 30s window

is considered: [155s; 185s]. The calculation procedure applied to the second assimilation window leads to the values of α = 0.0219 kW/s^2, t_0 = -66 s and λ_c = 0.53. The lead time is t_{lead} = 280 – 185 s = 95 s. Figure 12 shows the forecasting results for Test 3.

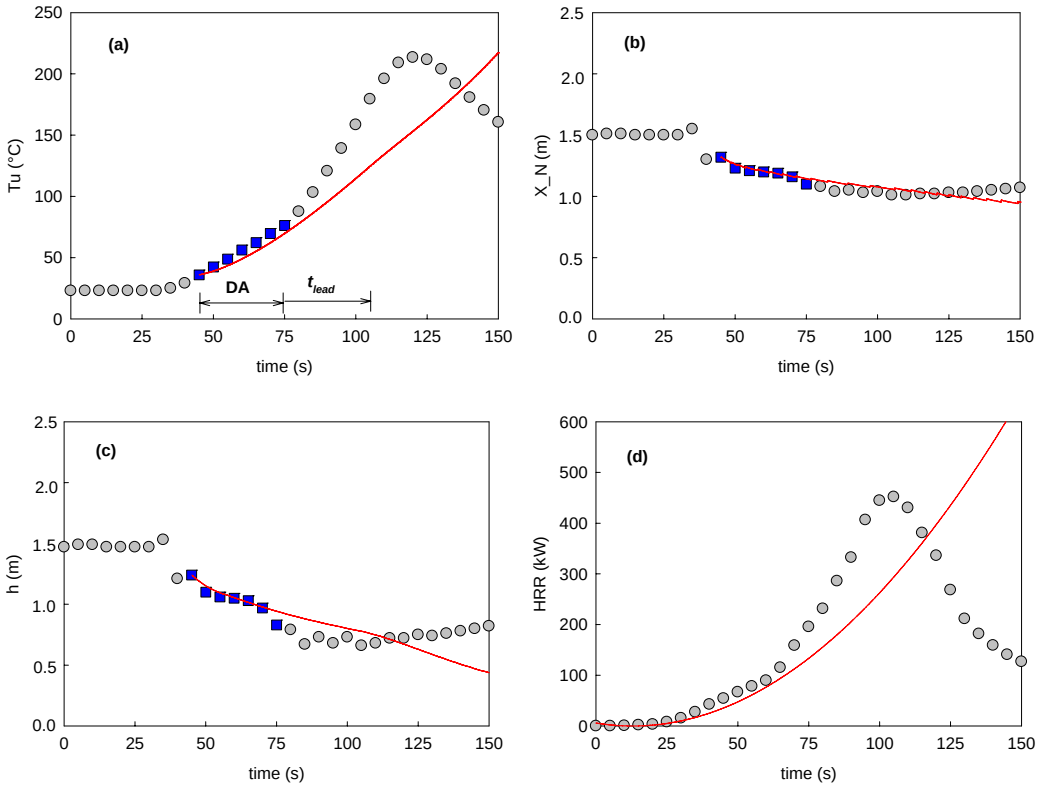

Figure 11. Test 2 fire forecast (solid line). The solid squares are the assimilated data points. The solid points are the remaining experimental data points. (a) Upper layer temperature. (b) Neutral Plane height. (c) Smoke layer height. (d) HRR.

In Test 4, the first assimilation window considered is [35s; 65s]. The optimized values are: α = 0.0007 kW/s^2, t_0 = -65 s and λ_c = 0.00. From t = 300 s onward the neutral plane height is systematically overestimated and the temperature underestimated by more than 50°C.

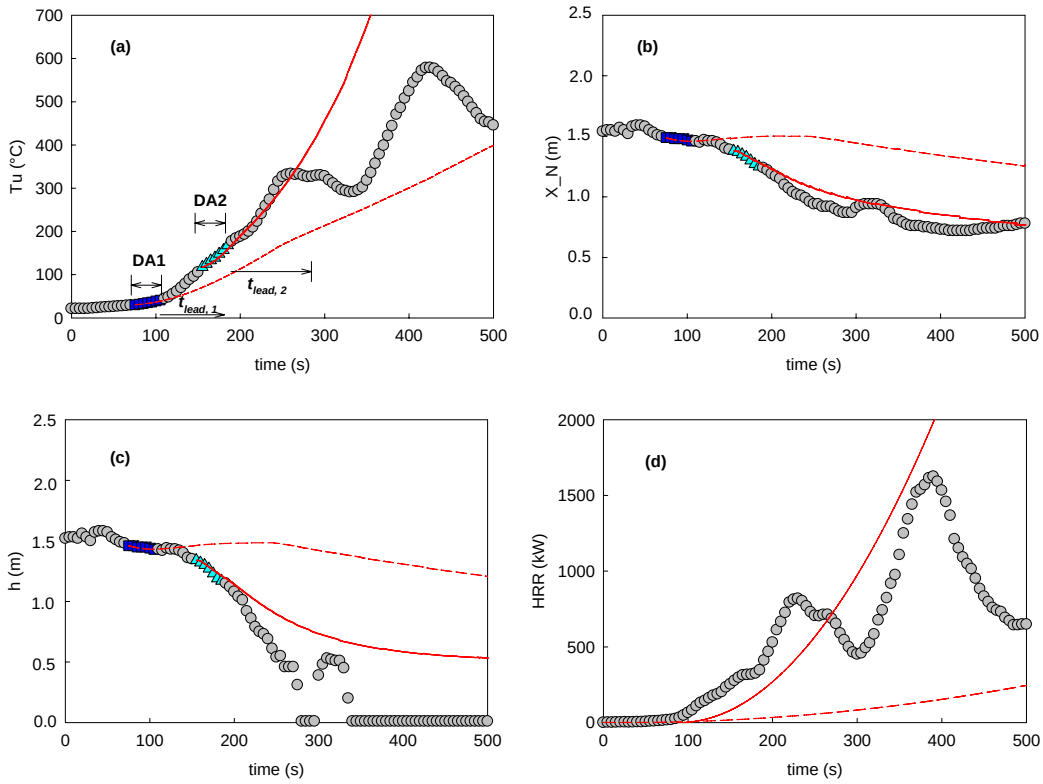

Figure 12. Test 3 fire forecasts. First forecast: dashed line. Second forecast: solid line. The solid squares are the first set of assimilated data points. The solid triangles are the second set of assimilated data points. The solid points are the remaining experimental data points. (a) Upper layer temperature. (b) Neutral Plane height. (c) Smoke layer height. (d) HRR.

Therefore, the lead time obtained after the first assimilation is t_{lead} = 300 – 65 s = 235 s. A new 30s window is considered: [285s; 315s]. The calculation procedure applied to the second assimilation window leads to the values of α = 0.0586 kW/s^2, t_0 = -70 s and λ_c = 0.58. The lead time is t_{lead} = 335 – 315 s = 20 s. Figure 13 shows the forecasting results for Test 4. An additional inverse modelling procedure using a linear growth model is applied for Test 4. The results shown in Fig. 14 demonstrate that the proposed forecasting methodology is not sensitivite to the growth model in this test.

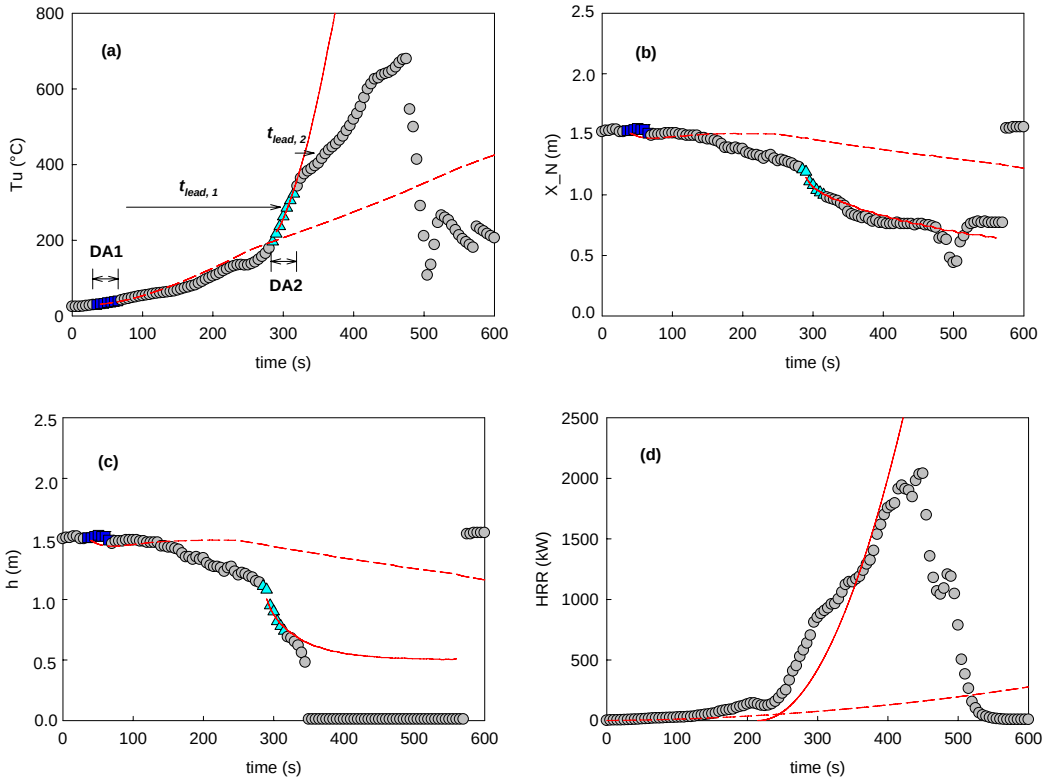

Figure 13. Test 3 fire forecasts. First forecast: dashed line. Second forecast: solid line. The solid squares are the first set of assimilated data points. The solid triangles are the second set of assimilated data points. The solid points are the remaining experimental data points. (a) Upper layer temperature. (b) Neutral Plane height. (c) Smoke layer height. (d) HRR.

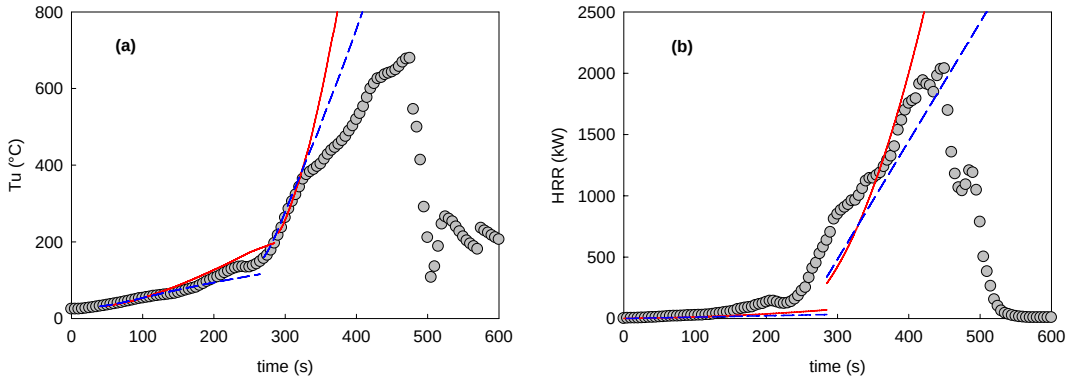

Figure 14. A comparison in the predictions of (a) upper layer temperature and (b) HRR for Test 4 using a quadratic growth model (solid line) or a linear growth model (dashed line).

CONCLUSIONS

A methodology developed for effectively forecasting fire growth based on assimilation of sensor observations has been applied to actual fire experiments in an ISO-room. Regarding the sensing part, good agreement between thermocouple data and video data has been achieved for the smoke layer height. Transient profiles of neutral plane height and temperature at the doorway level are assimilated in a two-zone model, chosen for its ability to convey instantaneously (thanks to the simple formulation) the tenability conditions induced by a compartment fire (in the pre-flashover stage). Inverse fire modelling over a limited period of time (*i.e.* assimilation window) in conjunction with a quadratic fire growth fit allows the instantaneous display of a forecast. The latter is subject to dynamic updating when necessary. The encouraging results obtained allow further numerical and experimental testing for more complex fire scenarios, including multi-compartment fires and scenarios with sudden changes in the fire conditions (such as different ventilation conditions or secondary object ignition).

ACKNOWLEDGMENTS

The research activities as described in this paper were funded by Ghent University, the Interdisciplinary Institute for Broadband Technology (IBBT), University College West Flanders, WarringtonFireGent, the Institute for the Promotion of Innovation by Science and Technology in Flanders (IWT), the Fund for Scientific Research-Flanders (FWO-Flanders G.0060.09), the Belgian Federal Science Policy Office (BFSPO), and the European Union.

NOMENCLATURE

C_d discharge coefficient

c_p specific heat of air

g	gravitational acceleration (m/s^2)
H	height of the room (m)
H_D	doorway height (m)
h	smoke layer height from floor level (m)
$\dot{m}$	mass flow rate (kg/s)
N	number of measurements in the assimilation window
N_{data}	total number of measurements
$\dot{Q}_f$	total heat release rate of the fire (kW)
$\dot{Q}_{net}$	net heat release rate (kW)
T	temperature (K)
t	time (s)
t_0	delay time (s)
W_D	doorway width (m)
X_N	neutral plane height (m)
z_f	elevation of the fire source above floor level (m)
λ_c	heat loss factor
ρ	density (kg/m^3)

Subscripts

a	ambient conditions
i	measurement index
in	gas flow inside the room
l	lower layer
net	quantity related to the fraction of energy heating the upper layer
out	gas flow outside the room
p	plume
u	upper layer

REFERENCES

[1] Cowlard A., Jahn W., Abecassis-Empis C., Rein G. (2010). Sensor Assisted Fire Fighting, Fire Technol., 46:719-741.

[2] Jahn W., Rein G., Torero J.L. (2010). Forecasting fire growth using an inverse zone modeling approach, Fire Safety J., 46:81-88.

[3] Jahn W. (2010). Inverse Modelling to Forecast Enclosure Fire Dynamics, PhD Thesis, The University of Edinburgh. http://hdl.handle.net/1842/3418.

[4] Beji T., Verstockt S., Van de Walle R., Merci B. (2012). Prediction of smoke filling in large volumes by means of data assimilation-based numerical simulations, J. Fire Sci., 30:300-317.

[5] ISO 9705, International Standard, "Fire Tests - Full Scale Room Test for Surface Products", First Edition, Reference Number ISO/TC92/WG7/N124, 1993.

[6] Davis W.D., Forney G.P., A sensor-driven fire model version 1.1, National Institute of Standards and Technology, Building and Fire Research Laboratory, Gaithersberg, MD 20899-8642, NISTIR 6705, 2001. http://fire.nist.gov/bfrlpubs/fire01/PDF/f01002.pdf.

[7] Peacock R.D., McGrattan K.B., Klein B., Jones W.W., Reneke P.A., CFAST – Consolidated Model of Fire Growth and Smoke Transport (Version 6): Software Development and Model Evaluation Guide. Special Publication 1086, National Institute of Standards and Technology, Gaithersburg, Maryland, 2008. http://fire.nist.gov/bfrlpubs/fire05/PDF/f05114.pdf.

[8] Neviackas A.W. (2007). Inverse fire modeling to estimate the heat release rate of compartment fires, Master's thesis, University of Maryland. http://hdl.handle.net/1903/7290.

[9] McGrattan K., Klein B., Hostikka S., Floyd J., Fire Dynamics Simulator (Version 5)-User's Guide. NIST Special Publication 1019-5, 2008.

[10] T. Tanaka, S. Yamada (2004), 'BRI2002: Two layer zone smoke transport model', Fire Science and Technology 23 (1) Special Issue.
https://www.jstage.jst.go.jp/article/fst/23/1/23_1_1/_pdf

[11] Koo S.H., Fraser-Mitchell J., Welch S. (2010). Sensor-steered fire simulation, Fire Safety J., 45:193-205.

[12] Zukoski E., Development of a stratified ceiling layer in the early stages of a closed-room fire, Fire and Materials 2 (2). doi: 10.1002/fam.810020203.

[13] Overholt K.J., Ezekoye, O.A. (2012), Characterizing heat release rates using an inverse fire modeling technique, Fire Technol. doi: 10.1007/s10694-011-0250-9.

[14] Beji T., Verstockt S., Van de Walle R., Merci B. (2012). On the Use of Real-Time Video to Forecast Fire Growth in Enclsoures, Fire Technol.. doi: 10.1007/s10694-012-0262-0.

[15] Verstockt S., Van Hoecke S., Tilley N., Merci B., Sette B., Lambert P., Hollemeersch C., Van de Walle R. . (2011). FireCube: a multi-view localization framework for 3D fire analysis, Fire Safety J., 46: 262-275.

[16] Walton W.D. (1985). ASET-B: a room fire program for personal computers, Fire Technol., 21: 293-309.

[17] Brani D.M., Black W.Z. (1992). Two-Zone Model for a Single-Room Fire, Fire Safety J., 19:189-216.

[18] Cooper L.Y. (1982), A mathematical model for estimating available safe egress time from fires, Fire Mater., 6:135-143.

[19] Cooper L.Y., Compartment fire-generated environment and smoke filling, in: DiNenno PJ, Editor-in-Chief, SFPE handbook of fire protection engineering, 2nd ed., Quincy, MA: National Fire Protection Association, pp.3-174-96, 1995.

[20] Mowrer F.W. (1999). Enclosure smoke filling revisited, Fire Safety J., 33:93-114.

[21] Hamins A., Johnsson E., Donnelly M., Maranghides A., Energy balance in a large compartment fire (2008). Fire Safety J., 43:180-188.

[22] McCaffrey B.J. (1983). Momentum implications for buoyant diffusion flames, Combust. Flame 52:149-67.

[23] Heskestad G., Fire plumes, flame height and air entrainment, in: DiNenno PJ, Editor-in-Chief, SFPE handbook of fire protection engineering, 3rd ed., Quincy, MA: National Fire Protection Association, 1995. pp.3-174-196, NFPA, 2-1–2-17, 2002.

[24] Zukoski E.E., Kubota T., Cetegen B. (1981). Entrainment in fire plumes, Fire Safety J., 3: 107-121.

[25] Thomas P.H., Hinkley P.L., Theobald C.R.,. Simms D.L (1963). Investigations into the flow of hot gases in roof venting. Fire Research Technical Paper No. 7, London, The Stationary Office.

[26] Dembsey N.A., Pagni P.J., Williamson R.B. (1995). Compartment Fire Near-Field Entrainment Measurements, Fire Safety J., 24:383-419.

[27] Karlsson B., Quintiere J., Enclosure Fire Dynamics, CRC press, 2000.

[28] He Y., Fernando A., Luo M. (1998). Determination of interface height from measured parameter profile in enclosure fire experiment, Fire Safety J. 31:19-38.

[29] Steckler K.D., Quintiere J.G., Rinkinen W.J. (1982). Flow induced by fire in a compartment, Nineteenth Symposium (International) on Combustion / The Combustion Institute, 19:913-920.

[30] Friedman R., Quantification of threat from a rapidly growing fire in terms of relative material properties (1978), Fire Mater., 2:27–33.

[31] Mizuno T., Kawagoe K. (1984). Burning behavior of upholstered chairs, Part I, Fire Sci. Technol., 4:37-45.

[32] Delichatsios M.A. (1976). Fire growth rates in wood cribs, Combust. Flame 27: 267-278.

[33] Heskestad G., Delichatsios M. A. (1979). The initial convective flow in fire, Seventeenth Symposium (International) on Combustion. The Combustion Institute, Pittsburgh, PA, 38 (6) 1113-1123. http://dx.doi.org/10.1016/S0082-0784(79)80106-X.

[34] Babrauskas V., Walton W.D. (1986). A Simplified Characterization of Upholstered Furniture Heat Release Rates, Fire Safety J., 11:181 – 192.